AGH DRILLING, OIL, GAS • Vol. 32 • No. 4 • 2015

http://dx.doi.org/10.7494/drill.2015.32.4.657

Ewa Knapik*, Damian Janiga*, Paweł Wojnarowski*, Jerzy Stopa*

THE ROLE OF CAPILLARY TRAPPING DURING GEOLOGIC CO_2 SEQUESTRATION**

1. INTRODUCTION

CO_2 injection to depleted deposits and aquifers is a common method of limiting CO_2 content in the atmosphere. Aside from a positive environmental impact, CCS is of great industrial significance when combined with enhanced oil recovery (EOR) methods. Generally speaking, there are four CO_2 fixing mechanisms in the porous medium: stratigraphic/structural trapping, dissolution trapping, residual (or capillary) trapping and mineral trapping [1]. Stratigraphic trapping occurs when free gas CO_2 migrates towards the top of the formation as a result of the buoyancy force and accumulates there in the form of the gas cap [2]. The cap rock of the structure plays a key role; to maintain storage integrity, injection pressure cannot exceed the fracture pressure. The storage capacity depends on available free pore space, thus it is beneficial to inject to the depleted deposits of hydrocarbons. Additionally, the depleted deposits are well-recognized in terms of petrophysical and geomechanical parameters, thanks to which it is easy to model CO_2 migration in the subsurface. CO_2 dissolution in the brine leads to the emergence of brine of high density, which sinks in the reservoir in the form of thick and thin fingers. This phenomenon is called dissolution trapping. The dissolution process occurs very slowly, Kampman et al. [3] estimates that the rate of CO_2 penetration into static brine is about 25 cm per year. A physical mechanism of the process is based on three phenomena: molecular diffusion of CO_2 into brine, dispersion during flow and convection of CO_2-saturated (heavier) brine in the formation. CO_2 solubility rises with increase of deposit pressure but drops with increase of temperature and brine salinity [4]. Carbonic acid formation results in dissolution of reservoir salts and precipitation of minerals, which leads to a permanent CO_2 fixing in the deposit, that is the so-called mineral trapping. Predicting the

* AGH University of Science and Technology, Faculty of Drilling, Oil and Gas, Krakow, Poland

** The research leading to these results has received funding from the Polish-Norwegian Research Programme operated by the National Centre for Research and Development under the Norwegian Financial Mechanism 2009–2014 in the frame of Project Contract No Pol-Nor/235294/99/2014

effective mineral trapping capacity of a reservoir is a complex problem due to the opposite CO_2 – cap rock interactions under geosequestration conditions. Mineral dissolution includes both direct dissolution of carbonates and hydrolysis of feldspars and phyllosilicates and increases permeability which also enhances the trapping process [5]. In contrast, precipitation of carbonate minerals may significantly reduce rock permeability by blockage of small pore throats. The kinetics of these phenomena varies over wide range, from a few weeks for gas adsorption onto the rock matrix to hundreds of years for minerals precipitation. Due to the complexity of the CO_2-brine-porous medium interactions, it is difficult to identify the dominant mechanism and on this basis forecast for the security of the entire storage. In general, solubility and mineral trapping are considered as long-term processes that ensure the complete and permanent immobilization of CO_2 in the deposit.

Physical properties of the rock mass, in particular the size and distribution of pores and saturation with reservoir fluids play a vital role in the case of capillary trapping. From the point of view of the fluid mechanics, this phenomenon is highly interesting and in the last couple of years a set of studies have been conducted in order to explain it. The results of laboratory tests and a mathematical model for capillary trapping during CO_2 storage have been described below.

2. PORE SCALE PROCESSES UNDERLYING CAPILLARY TRAPPING

For geologic carbon sequestration, two different displacement regimes, namely drainage and imbibition, are observed [7–11]. Drainage refers to the decreasing saturation of a wetting phase. Imbibition occurs when the wetting-phase saturation increases. During the injection period CO_2 displaces the brine from the pore space in a drainage-like process. The only mechanism for drainage stage is a piston-type displacement. However, water is still present in small pores that have not been filled with CO_2 and in the corners of the pore space, with the non-wetting phase initially in the centre. After completion of the injection the gas is displaced by brine and forming a vertical path migrates towards the top of formation due to the buoyant force and the density difference – imbibition phase. System wettability determines fluid distribution on the pore scale [6–7]. Typically brine is a wetting phase for the rock matrix and during displacement gas bubbles (non-wetting phase) are trapped in small clusters of pores as an immobile phase (Fig. 1a). The increase of water pressure causes the water layers to expand and fill the narrower regions, called throats. CO_2 bubbles are pushed out of the narrower regions and trapped in larger pores, which is referred to as snap-off [8]. In the case of rocks which are water-wet (contact angle values measured through the aqueous phase vary from 0° to 90°), the potential flow occurs easier due to minor resistance, and snap-off effect is increased. According to the theory of percolation [8], the biggest pores are first to be filled with water, thus large pores and relatively smaller throats favor trapping. The snap-off mechanism may be reduced or eliminated entirely in intermediate-wet media.

For these two displacement regimes the hysteresis between the receding (Q_r, in drainage) and advancing contact angle (Q_a, in imbition) occurs. The relative permeability and capillary pressures depend on the saturation path and the saturation history [9]. Oak's studies [18] show that in the case of the water-wet porous medium for the wetting phase there is no relative permeability hysteresis or this effect is extremely low.

a) b)

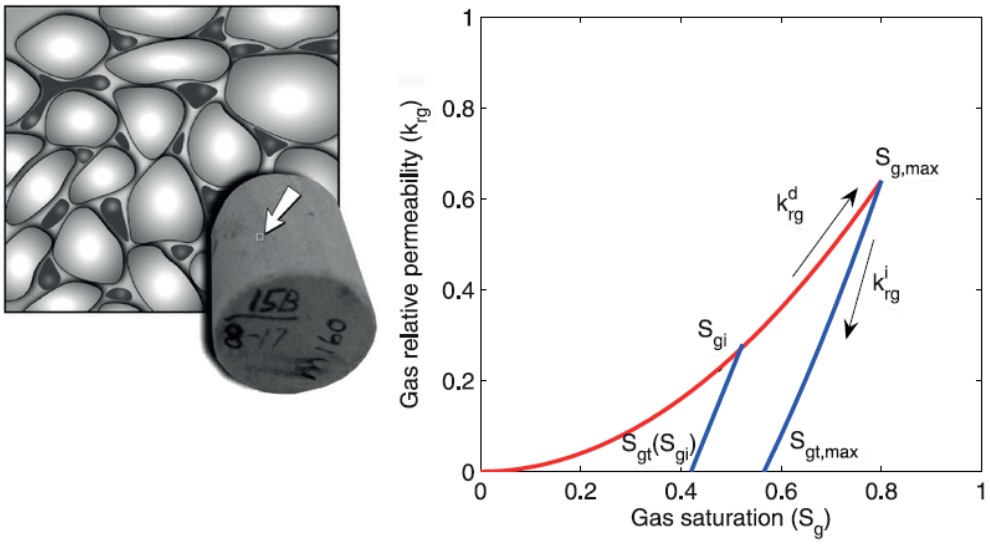

Fig. 1. Disconnected bubbles of non-wetting gas in a water-wet porous medium [1] (a); relative permeability of CO_2 for a water wet Berea sandstone [9] (b)

In turn, for the non-wetting phase, i.e. the CO_2 hysteresis effect is conspicuous. The trapped (residual) gas saturation applies to the CO_2 saturation value at the end of imbibition phase and determines the amount of permanently fixed CO_2.

Trapped gas saturation, S_{gt}, can be calculated in accordance with the Land's equation [9]:

$$S_{gt} = \frac{S_{gi}}{1 + C \cdot S_{gi}} \tag{1}$$

where S_{gi} is the initial gas saturation (actual at flow reversal). The Land trapping coefficient, C, is defined as:

$$C = \frac{1}{S_{gt,\max}} - \frac{1}{S_{g,\max}} \tag{2}$$

where $S_{g,\max}$ is the highest gas saturation at the drainage stage possible to achieve, and $S_{gt,\max}$ is the maximum trapped saturation, associated with the bounding imbibition curve (see Fig. 1b). Basically, the higher the CO_2 saturation, the higher the residual saturation at the end of the drainage period after water flooding, the relationship between the initial and residual non-wetting saturations is known as the IR (for the initial-residual) curve. The Brooks–Corey model is often used to describe the relative permeability for a two-phase system [19]:

$$k_{rw} = (S_w^*)^{\frac{2+3\lambda}{\lambda}} \tag{3}$$

$$k_{rg} = (1 - S_w^*)^2 \left(1 - (S_w^*)^{\frac{2+3\lambda}{\lambda}}\right) \tag{4}$$

$$(S_w^*) = \frac{S_w - S_{wir}}{1 - S_{wir}} \tag{5}$$

where: k_{rw} i k_{rg} are relative permeability for water and gas, respectively; S_w – current saturation with water, S_{wir} residual saturation with water, λ is the pore size distribution index.

Bennion and Bachu [20] indicated the relative permeability curves for different rock samples from the Wabamun and Zama areas, Alberta, Canada.

Table 1

The in-situ conditions and rock characteristics for relative permeability measurements [20]

Rock sample	Lithology	Porosity [%]	S_{gt} (trapped gas)	Corey-model parameter for brine	Corey-model parameter for CO_2	P [MPa]	T [°C]
Viking	sandstone	19.5	0.297	2.1	4.0	8.6	35
Calmar	shale	3.9	0.256	4.0	2.2	12.25	43
Nisku	carbonate	11.4	0.218	2.1	4.4	17.4	56
Muskeg	anhydrite	1.2	0.18	n/a	n/a	15	71

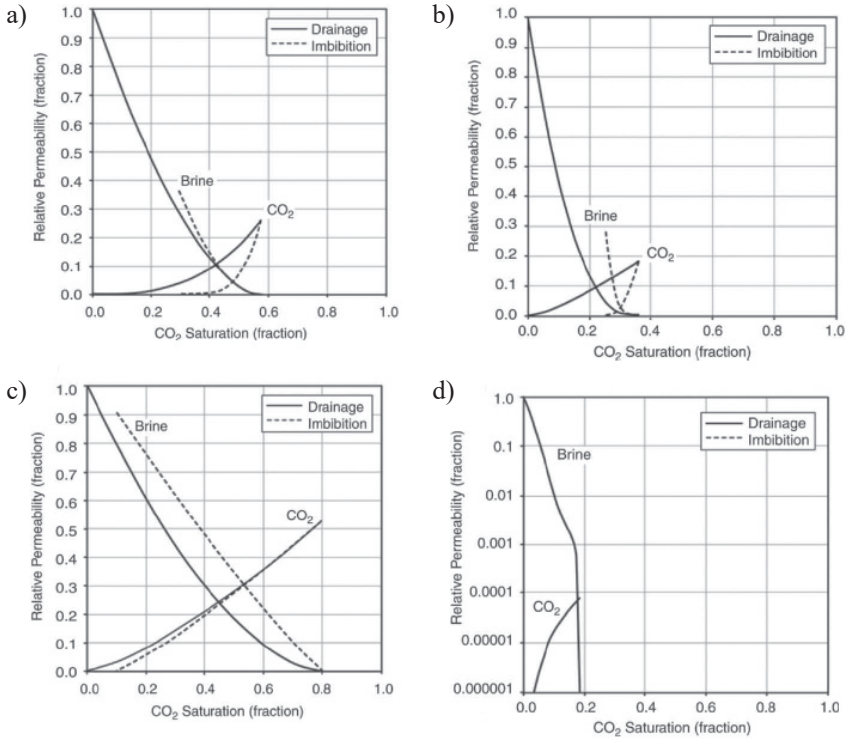

Fig. 2. Relative permeability curves for CO_2/brine systems for in-situ conditions for the following core samples: a) Viking; b) Calmar; c) Nisku; d) Muskeg [20]

High permeability assures easy CO_2 flow from the wells inside the formation (possible low bottom pressure) on the one hand, and facilitates displacement of CO_2 by water at the imbibition phase on the other. On the contrary, low vertical permeability hinders CO_2 escape towards the top of the structure as a result of the buoyancy force. The type of rock has a considerable influence on reservoir storage capacity. Due to their low porosity and extremely low permeability, anhydrites and shale have low critical CO_2 saturation at the drainage phase, but since water displacement is hindered, the final residual saturation remains at the level of 20%. It is thought that carbonates can be a promising storage area of CO_2 because it is possible to precipitate CO_2 in the form of minerals, but a system of double porosity (cracks and pores) can pose a hazard of uncontrolled leak.

Apart from the relative permeability hysteresis, one observes that the capillary pressure–saturation relationships also exhibit marked hysteresis effects. Yet, from the point of view of computer modeling of CO_2 migration in the reservoir, the capillary effects can be neglected because as a rule the characteristic capillary length is much smaller than the grid resolution [9].

The storage capacity of the porous medium resulting from the capillary trapping phenomenon, C_{trap}, depends on the residual CO_2 saturation and porosity, in accordance with the following equation:

$$C_{trap} = \varphi \cdot S_{gt} \tag{6}$$

where:

φ – porosity,
S_{gt} – trapped CO_2 saturation.

Iglauer et al. [10] studies suggest that the maximum storage capacity is achieved when the deposit porosity equals 20–30%. The lower the porosity, the smaller the geometric space for fluids. High-porosity, unconsolidated media exhibit better connected pore spaces giving lower residual saturations. Pore-size distribution affects CO_2 relative permeability, microporosity enhances a more uniform displacement character.

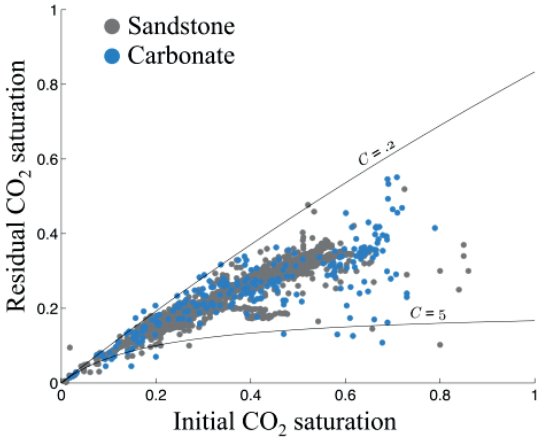

Fig. 3. Reported observations of residual trapping with supercritical CO_2 [8]

3. INFLUENCE OF OPERATING PARAMETERS ON CAPILLARY TRAPPING EFFECTIVENESS

Numerous parameters determine migration and CO_2 retention in the reservoir, including capillary, viscous and gravitational forces. Dependencies between them are described by dimensionless numbers specified below [11]:

Capillary number, Ca, describes the relation of viscous to capillary forces:

$$\mathrm{Ca} = \frac{\mu_i \cdot \nu}{\sigma \cdot \cos\Theta} \tag{7}$$

where:

μ – viscosity of the invading fluid,
ν – superficial velocity of the invading fluid,
σ – interfacial tension between the two fluids,
Θ – contact angle.

The viscosity ratio, M, is used to compare the viscosities of the invading and displaced fluids, and defined as:

$$M = \frac{\mu_i}{\mu_d} \tag{8}$$

where μ_i, μ_d are the viscosities of the invading and displaced fluids, respectively.

The effects of gravity on the system can be described by the Bond number (Bo), which is typically defined as [6]:

$$\mathrm{Bo} = \frac{gravity\ forces}{capillary\ forces} = \frac{\Delta\rho \cdot g \cdot d^2}{\sigma \cdot \cos\Theta} \tag{9}$$

where $\Delta\rho$ is the density difference between the invading and displaced fluids, g is the gravitational constant, d is a representative length scale (the median bead or grain diameter).

The three distinct flow regimes could be identified: viscous fingering, capillary fingering, and stable displacement [19–21]. The residual non-wetting phase saturation depends on the capillary number during the imbibition stage. For very slow (quasi-static) displacements (that is low Ca values) capillary forces play a significant role in the system, they prevent the non-wetting phase from penetrating a porous medium. CO_2 can only enter a pore throat when the pressure in the non-wetting fluid exceeds the pressure in the wetting fluid by a value of capillary pressure. The displacement depends on the pore size distribution. The observed structures at the pore-network level consist of a rough and wide front which penetrate the largest pore throat accessible. Cense and Berg [15] indicated that a capillary dominated behaviour occurs at capillary numbers that are typically of the order of $10^{-6} - 10^{-4}$. At higher capillary numbers a viscous fingering regime is observed. A rapid breakthrough of the non-wetting fluid into the wetting fluid occurs and the front morphology is dictated by the viscosity ratio [11–14]. During imbibitions, brine is more viscous than the displaced CO_2 ($M > 1$) and the stable displacement is observed. At drainage stage the invading fluid is less viscous ($M < 1$) and the front is destabilized. Long and thin viscosity fingers are formed, which results in a higher residual saturation of CO_2.

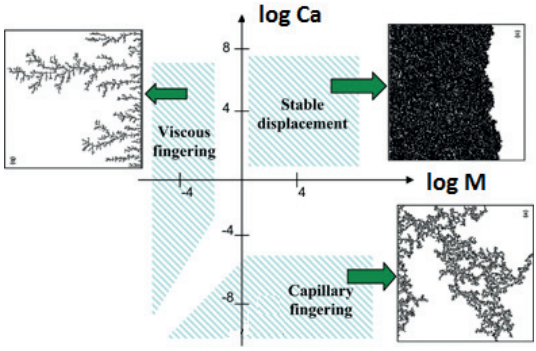

Fig. 4. Lenormand phase diagram: various transport regimes
and characteristic distribution of non-wetting phase for these regimes [12]

For the 3D system the displacement front behavior may be deduced using the generalized Bond number ($Bo^* = Ca - Bo$) [16]. For values of $Bo^* > 0$ the displacement front due to gravity is observed to evolve from narrow branched fingers to a nearly flat geometry. At Bo^* values in the range of $0 < Bo^* < -0.05$ capillary forces remain dominant and the front exhibits capillary fingering. For Bo^* lower than –0.08 viscous forces grow and gravity is not sufficient to prevent the viscous fingering.

In accordance with the definition of Ca and Bo numbers, deposit fluid properties have a significant impact on residual CO_2 saturation. CO_2-brine interfacial tension (IFT) depends on aquifer pressure, temperature and water salinity due to CO_2 solubility effects. Bachu and Bennion [17] found that IFT decreases for relatively low pressures (<10 MPa) as pressure increases, and displays an asymptotic behavior towards a constant value for higher pressures. The studies [17] have showed that increasing IFT values increase residual CO_2 saturations in consolidated sandstone samples collected from a site in Alberta, Canada. As the difference in density between CO_2 and brine increases, the non-wetting fluid is more likely to be mobilized upward, which leads to decreasing residual CO_2 saturation. The impact of viscosity on fluid flow in the deposit is defined by mobility ratio.

4. RESERVOIR MODEL

The simulation of CO_2 injection were carried out using a realistic model of geologic formation. The simulation objective is to illustrate the long-term impact of capillary trapping on storage capability. The formation is initially filled only with brine (aquifer). The reservoir model contains eight layers. The first four are a sand layers, the next one is a shale and layers six to eight represent the second sand complex. Reservoir parameters is shown in Table 2. The reservoir model is shown in Figure 5. The modeled formation is a typical anticline which from the point of view of gas injection is undesirable because a gas cap may be easily formed. The model has five injection wells open to the reservoir. The injection wells are group rate controlled and operated with a constrain in the maximum bottom hole pressure of 200 bar. The relative permeabilities were taken for Viking reservoir after reference [20] as may be seen in Figure 2. The relative permeability hysteresis in Eclipse 300 was modeled by the

Killough method [22]. In this method, the gas relative permeability along a scanning curve is computed as [9]:

$$k_{rg}^{i}(S_g) = k_{rg}^{ib}(S_g^*)\frac{k_{rg}^{d}(S_{gi})}{k_{rg}^{d}(S_{gi,\max})} \tag{10}$$

$$S_g^* = S_{gt,\max} + \frac{(S_g - S_{gt})(S_{gi,\max} - S_{gt,\max})}{S_{gi} - S_{gt}} \tag{11}$$

where k_{rg}^{d} and k_{rg}^{ib} represent the bounding drainage and imbibition curves, respectively.

Reservoir conditions ensure that the CO_2 is present as a supercritical fluid. The CO_2 injection is started at the bottom layer (6–8) using wells from I1 to I5. The injection period is 10 years. Well I3 is both an injection and observation well because of its location near to the top of the anticline structure (location of observation cell: 22, 21, 1 – 8). Two different scenarios were simulated: case 1 without relative permeability hysteresis and the second case within hysteresis. For each case the results of the fluid distribution are shown in Figure 6–8.

Table 2

Reservoir parameters

Model dimension (nx × ny × nz)	40 × 35 × 8	Cell
Average porosity	20	[%]
Average horizontal permeability	75	[mD]
Average thickness	144	[m]
Formation top	850	[m]
Reservoir pressure	110	[bar]
Reservoir temperature	322	[K]

Migration of CO_2 to the top is relatively fast, after 20 years from the start of injection the saturation of CO_2 in the upper layers is approx. 60%. In the first case, the gravity segregation of immiscible fluids leads to drastic changes in saturation of the lower layers, at the beginning of the injection the saturation of CO_2 is at the level of 55% and after 83 years drops to less than 10%. Taking into account the hysteresis (case 2) the CO_2 saturation distribution in layers is more uniform, the average saturation of the layer is approx. 30%. Capillary trapping thus leads to better use of storage space.

The capillary trapping process is sensitive to a set of various factors. Reservoir conditions, i.e. pressure and temperature, have a considerable impact on interfacial tension and the mobility ratio, and these in turn determines relative permeability, irreducible water and CO_2 saturations.

The observation points were chosen along well I3. The observation grid blocks is shown in Figure 9. Figure 10 shows the dynamic movement of CO_2 in the simulated region in terms of CO_2 phase saturations.

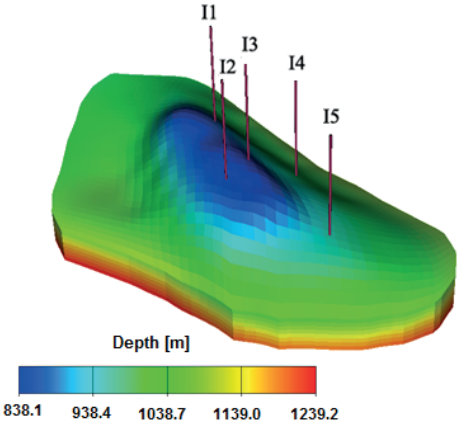

Fig. 5. Reservoir model used to simulation CO_2 trapping

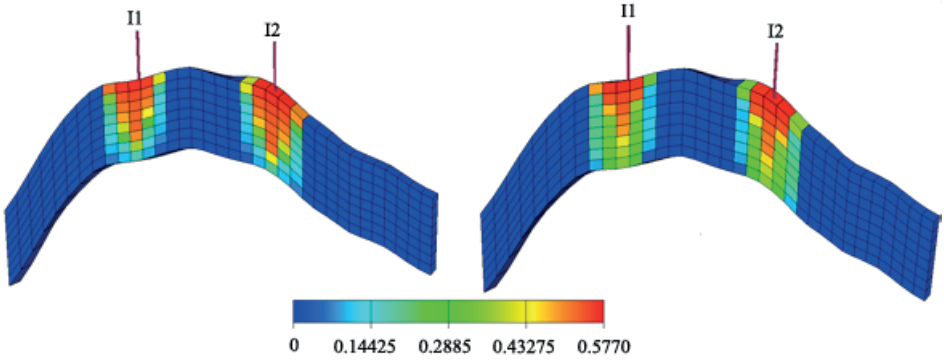

Fig. 6. CO_2 saturation distribution after 20 years from the beginning of injection for the reservoir vertical intersection. Results from case 1 (no hysteresis left).
Results from case 2 (with hysteresis right)

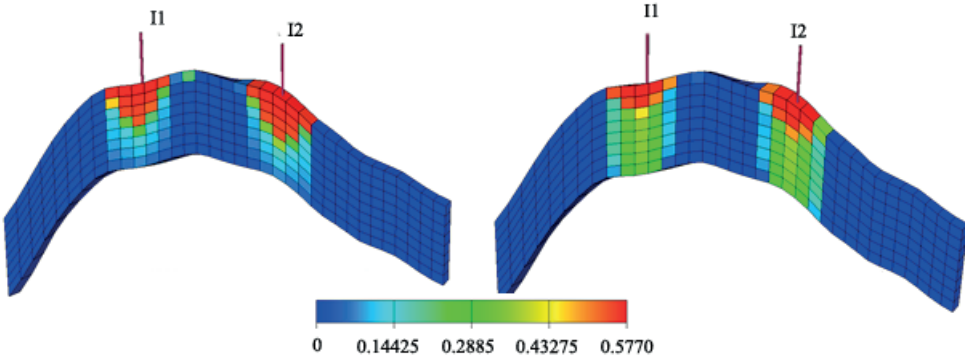

Fig. 7. CO_2 saturation distribution after 30 years from the beginning of injection for the reservoir vertical intersection. Results from case 1 (no hysteresis left).
Results from case 2 (with hysteresis right)

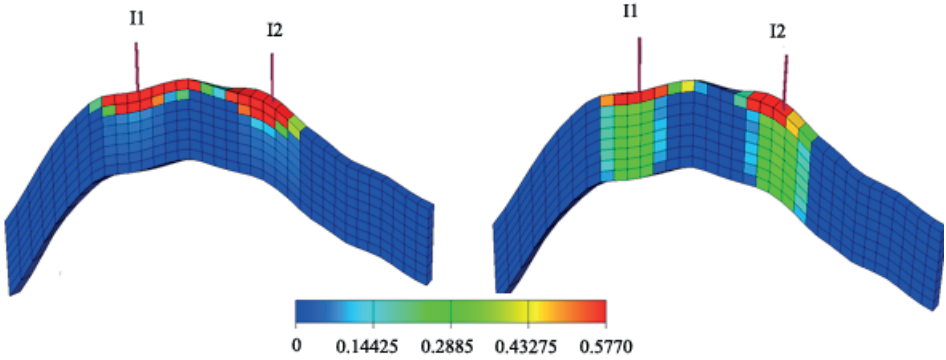

Fig. 8. CO_2 saturation distribution after 83 years from the beginning of injection for the reservoir vertical intersection. Results from case 1 (no hysteresis left).
Results from case 2 (with hysteresis right)

The saturation path for the top layer (observation point 1) is the same in both cases, after 20 years the saturation of CO_2 reaches the maximum value. In the scenario 1 the CO_2 saturation remains high, up to 50%, for the second and third layer and for layers below is

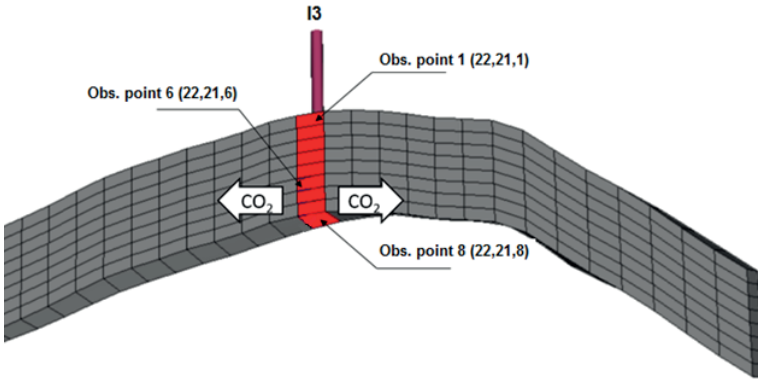

Fig. 9. Location of observation and injection points

low (approx. 10%). Within the hysteresis the saturation of CO_2 drops to 45% (layers 2–3) and for the other layers remains at the level of 30%. Simulations showed that the residual gas saturation is up to 30%. This result complies with previous works of Juanes et al. [9] and Bennion et al. [20]. The individual layers slightly differ in permeability, hence the time after which the layer saturation reaches a constant level varies, generally after 50 years no spontaneous movement of fluids is observed. Capillary trapping may be considered as dominant storage mechanism at early stage of geosequestration, dissolution and mineral trapping are considered as long-term processes.

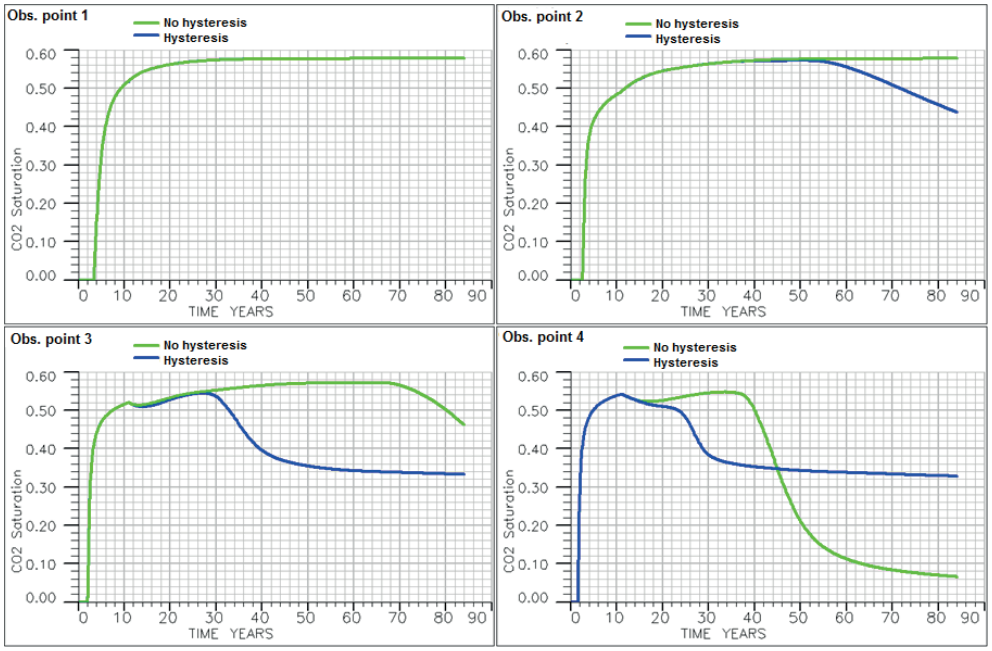

Fig. 10. Changes of CO_2 saturation in observation points

5. CONCLUSIONS

Capillary trapping of the CO_2 determines the migration and distribution of CO_2 in aquifers. On small timescales (<100 years) the capillary trapping becomes a dominant storage mechanism. In the model without hysteresis any trapping of CO_2 occurs which is unfavorable for sequestration purposes. A higher amount of CO_2 reaches the top of the anticline as a mobile phase and is prone to leaks. Trapping of the CO_2 due to relative permeability hysteresis leads to the situation where a large fraction of the CO_2 is trapped and immobile and is more spread out throughout the aquifer. From Figure 10 it can be deduced that up to 60% (residual CO_2 saturation/ initial CO_2 saturation, in percent) of injected CO_2 is trapped by capillary trapping mechanism. The process can be effectively simulated using commercial software by implementation of a proper model for the relative permeability hysteresis.

REFERENCES

[1] Bachu S.: *CO_2 storage in geological media: Role, means, status and barriers to deployment*. Progress in Energy and Combustion Science, vol. 34, 2008, pp. 254–273.

[2] Song J., Zhang D.: *Comprehensive review of caprock-sealing mechanisms for geologic carbon sequestration*. Environmental Science & Technology, vol. 47, 2012, pp. 9–22.

[3] Kampman N., Bickle M., Wigley M., Dubacq B.: *Fluid flow and CO_2-fluid-mineral interactions during CO_2-storage in sedimentary basins*. Chemical Geology, vol. 369, 2014, pp. 22–50.
[4] Adamczyk K., Premont-Schwarz M., Pines D., Pines E., Nibbering E.T.J.: *Real-time observation of carbonic acid formation in aqueous solution*. Science, vol. 326, 2009, pp. 1690–1694.
[5] Black J.R., Carroll S.A., Haese R.R.: *Rates of mineral dissolution under CO_2 storage conditions*. Chemical Geology, vol. 399, 2015, pp. 134–144.
[6] IPCC (Intergovernmental Panel on Climate Change), in: Metz B., Davidson O., de Coninck H.C., Loos M., Mayer L.A. (eds). *Special report on carbon dioxide capture and storage*. Cambridge University Press, Cambridge, UK – New York, USA 2005.
[7] Pentland C.H., El-Maghraby R., Georgiadis A., Iglauer S., Blunt M.J.: *Immiscible displacements and capillary trapping in CO_2 storage*. Energy Procedia, vol. 4, 2011, pp. 4969–4976.
[8] Krevor S., Blunt M.J., Benson S.M., Pentland C.H., Reynolds C., Al-Menhali A., Niu B.: *Capillary trapping for geologic carbon dioxide storage – From pore scale physics to field scale implications*. International Journal of Greenhouse Gas Control, vol. 40, 2015, 221–237.
[9] Juanes R., Spiteri E.J., Orr F.M. Jr, Blunt M.J.: *Impact of relative permeability hysteresis on geological CO_2 storage*. Water Resources Research, vol. 42, 2006, article number: W12418.
[10] Niu B., Al-Menhali A., Krevor S.C.: *The impact of reservoir conditions on the residual trapping of carbon dioxide in Berea sandstone*. Water Resources Research 2015 (in press).
[11] Kimbrel E.H., Herring A.L., Armstrong R.T., Lunati I., Bay B.K., Wildenschild D.: *Experimental characterization of nonwetting phase trapping and implications for geologic CO_2 sequestration*. International Journal of Greenhouse Gas Control, vol. 42, 2015, pp. 1–15.
[12] Sinha P.K., Mukherjee P.P., Wang C.Y.: *Impact of GDL structure and wettability on water management in polymer electrolyte fuel cells*. Journal of Materials Chemistry, vol. 17, 2007, pp. 3089–3103.
[13] Løvoll G., Meheust Y., Maløy K.J., Aker E., Schmittbuhl J.: *Competition of gravity, capillary and viscous forces during drainage in a two-dimensional porous medium, a pore scale study*. Energy, vol. 30, 2005, pp. 861–872.
[14] Cottin C., Bodiguel H., Colin A.: *Drainage in two-dimensional porous media: From capillary fingering to viscous flow*. Physical Review E, vol. 82, 2010, pp. 046315.
[15] Cense A.W., Berg S.: *The viscous-capillary paradox in 2-phase flow in porous media*, in: International Symposium of the Society of Core Analysts. Shell International Exploration & Production, Noordwijk, The Netherlands 2009.
[16] Or D.: *Scaling of capillary, gravity and viscous forces affecting flow morphology in unsaturated porous media*. Advances in Water Resources, vol. 31, 2008, pp. 1129–1136.
[17] Bachu S., Bennion B.: *Effects of in-situ conditions on relative permeability characteristics of CO_2-brine systems*. Environmental Geology, vol. 54, 2008, pp. 1707–1722.
[18] Oak M.J.: *Three-phase relative permeability of water-wet Berea*. SPE Pap. 20183-MS, Society of Petroleum Engineers, Richardson, Tex, SPE/DOE20183 1990.

[19] Flett M., Gurton R., Taggart I.: *The function of gas–water relative permeability hysteresis in the sequestration of carbon dioxide in saline formations*. SPE Pap. 88485-MS, Society of Petroleum Engineers, Richardson, Tex 2004.
[20] Bennion D., Bachu S.: *Supercritical CO_2 and H_2S – brine drainage and imbibition relative permeability relationships for intercrystalline sandstone and carbonate formations*. SPE Europec/EAGE Annual Conference and Exhibition, 12–15 June 2006, Vienna, Austria.
[21] Meheust Y., Lovoll G., Maloy K.J., Schmittbuhl J.: *Interface scaling in a two-dimensional porous medium under combined viscous, gravity, and capillary effects*. Physical Review E, vol. 66, 2002, pp. 051601–051603.
[22] Killough J.E.: *Reservoir simulation with history-dependent saturation functions*. Society of Petroleum Engineers Journal, vol. 16, no. 1, 1976, pp. 37–48.